02,05,13

Superconducting spin-valve effect in heterostructures with ferromagnetic Heusler alloy layers

© A.A. Kamashev[1], N.N. Garif'yanov[1], A.A. Validov[1], Ya.V. Fominov[2,3], I.A. Garifullin[1]

[1] Zavoisky Physical-Technical Institute, FRC Kazan Scientific Center of RAS, Kazan, Russia
[2] L.D. Landau Institute for Theoretical Physics, Chernogolovka, Russia
[3] Laboratory for Condensed Matter Physics, HSE University, Moscow, Russia

E-mail: kamandi@mail.ru

Received April 29, 2022
Revised April 29, 2022
Accepted May 12, 2022

The transport properties of two types of spin valves are analyzed, in which the Heusler alloy $Co_2Cr_{1-x}Fe_xAl_y$ was used as one of the two ferromagnetic layers in the F1/F2/S structures. The Heusler alloy layer was used: 1) as a weak ferromagnet, in the case of the F2 layer; 2) as a halfmetal, in the case of the F1 layer. In the first case, a large classical effect of the superconducting spin valve ΔT_c was obtained, which was facilitated by a significant triplet contribution to the effect of the superconducting spin valve ΔT_c^{trip}. In the second case, a gigantic effect value ΔT_c^{trip} was found reaching 0.5 K.

Keywords: superconductivity, ferromagnetism, thin films, superconducting spin valve.

DOI: 10.21883/PSS.2022.09.54151.18HH

1. Introduction

Today, there is a huge theoretical and experimental interest in the creation and development of logic elements for superconducting spintronics (for example, see [1,2]). According to these articles, the most promising devices for use in quantum logic elements are heterostructures based on the superconductor/ferromagnet (S/F) [3] proximity effect. In particular, in 1997, Professor Beasley's group from the Stanford University [4] proposed a theoretical model of a superconducting spin valve (SSV), based on the fact that the degree of suppression of the Cooper pairs depends on the mutual orientation of the ferromagnetic layer magnetizations in the F1/F2/S structure. Thus, it becomes possible to control the transition temperature to the superconducting state (T_c) in such systems. At the same time, it should be noted that, according to article [4] T_c, with antiparallel (AP) orientation of magnetizations, T_c^{AP} turns out to be higher than with a parallel (P) orientation T_c^P. The physical meaning of this statement is that the average value of the exchange field, which acts on the system's Cooper pairs, is less for the AP-orientation of the magnetizations of F-layers than for the P-orientations.

Another possible variant of SSV, based on the S/F proximity effect, was proposed theoretically by Professor Tagirov [5] in 1999. This construction was somewhat different from the construction proposed in article [4], and assumed a three-layer system F1/S/F2.

For more than ten years, it has not been possible to experimentally implement the superconducting spin valve proposed by Professor Beasley's group. For the first time, the full effect of the superconducting spin valve was experimentally implemented in the CoO_x/Fe1/Cu/Fe_2/In system in 2010 by our group [6]. The magnitude of the effect was $\Delta T_c = 19$ mK for the width of the superconducting transition $\partial T_c \sim 7$ mK.

Fominov et al. in their article [7] developed a theory for F1/F2/S structures that allows one to consider cases of non-collinear mutual orientation between magnetizations of F-layers. In this article, it was shown that the quantum interference of the pair wave function of the Cooper pair reflected from both sides of the F2-layer in F1/F2/S structures can be both constructive and destructive. For the case of collinear magnetizations, it was shown in [7] that, depending on the thickness of the F2-layer, both direct and inverse SSV effects can be observed. We have experimentally shown the alternating behavior of the SSV effect in our article [8].

Fig. 1 schematically shows the operation of the classical SSV, where the quantum interference of the pair wave function of the Cooper pair is constructive. Here are two superconducting transitions with a width of ∂T_c, corresponding to the P- and AP-magnetization orientations of F1- and F2-layers. The magnitude of separation of these superconducting transitions is the magnitude of the SSV effect $\Delta T_c = T_c^{AP} - T_c^P$. In Fig. 1, the shaded rectangle is the working temperature zone of SSV. If, within the given rectangle at fixed temperature, the mutual orientation of the magnetizations of F-layers is changed from AP to P, then a complete switching between the superconducting and normal states of the SSV will be observed. Thus, the width of this rectangle ΔT_c^{full} is the most important SSV

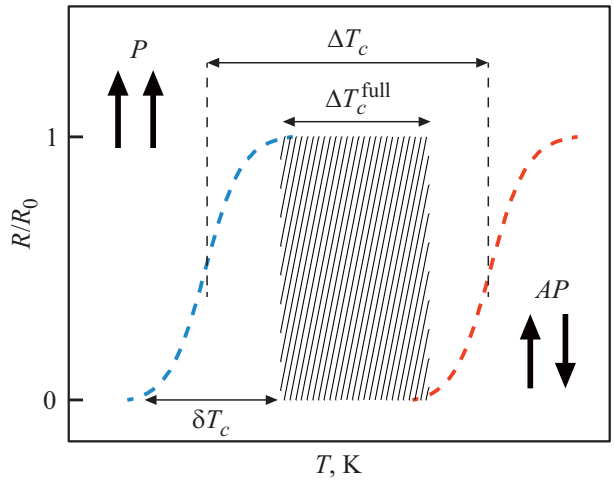

Figure 1. Schematic representation of the SSV operating principle. The dashed lines show the curves of superconducting transitions (resistivity ratio R/R_0 as a function of T) with width ∂T_c for parallel and antiparallel orientation of the magnetizations of F-layers. The shaded area ΔT_c^{full} wide shows the working area of SSV (see text).

parameter. It should be noted that the fulfillment of the condition $\Delta T_c > \partial T_c$ is not always a sufficient indicator of SSV operation success. As a rule, the magnitude ΔT_c^{full} is less than ΔT_c due to the final value ∂T_c, and this difference increases as the value ∂T_c increases. In our first article [6], in which we managed to experimentally implement the full SSV effect, the magnitude ΔT_c^{full} was of the order of 10 mK. Thus, to improve SSV efficiency, it is necessary to increase the magnitude of ΔT_c^{full}. This has been undertaken in a large number of articles in various SSV constructions (for example, see reviews [9–11] and later publications [12–14]).

The theory of Fominov et al. in article [7] predicted the generation of long-range triplet components (LRTC) of a superconducting condensate in the F1/F2/S structures at non-collinear orientations of the magnetizations of the F-layers. According to this theory, the characteristic minimum T_c on the angular dependence $T_c(\alpha)$ (where α is the angle between the magnetizations of the ferromagnetic layers) is a direct evidence of LRTC generation in the F1/F2/S structures.

To date, a large number of studies of the SSV effect have shifted towards the study of LRTC of a superconducting condensate (see articles [15–24]). For example, Jara et al. in article [25] experimentally investigated the superconducting properties of the CoO/Co/Cu/Co/Nb structure. They provided clear evidence for the presence of LRTC in their structures and also observed good agreement between theory and experiment. We observed complete switching between the normal and superconducting states using the triplet contribution to the SSV effect in the CoO_x/Py1/Cu/Py2/Cu/Pb structure, where Py = $Ni_{0.81}Fe_{0.19}$ [26]. A similar result was observed by Gu et al. [27,28] for the Ho/Nb/Ho and Dy/Nb/Dy structures. The magnitude of the SSV effect in these structures reached about 400 mK in an external magnetic field of the order of 10 kOe.

In 2015 Singh et al. [29] found a giant triplet contribution of $\Delta T_c^{\text{trip}} \sim 0.6{-}0.8$ K (to the SSV effect, where $\Delta T_c^{\text{trip}} = T_c^P(\alpha = 0°) - T_c^{PP}(\alpha = 90°)$) in the CrO_2/Cu/Ni/MoGe structure, in which a semi-metal CrO_2 was used as the F1-layer. It should be noted that this is a record value of the difference in superconducting transition temperatures measured for parallel (P) and perpendicular (PP) orientations of the magnetizations of F-layers. Singh et al. state that the observation of the giant magnitude ΔT_c^{trip} is due to the use of a semi-metallic CrO_2 layer. In this regard, for the further development of SSV performance, it is necessary to check whether the conclusion made in article [29] is really valid for other semi-metallic compounds as the F-layers of SSV.

We selected the Heusler alloy $Co_2Cr_{1-x}Fe_xAl_y$ (hereinafter HA) as the ferromagnetic material for our SSV structures. This alloy has interesting properties. It can be a weak ferromagnet and a semi-metal depending on the preparation conditions. We have shown in the article [30] that HA films prepared at a substrate temperature $T_{sub} \sim 300$ K are weak ferromagnets (hereinafter HA^{RT}). If HA films are sputtered at the substrate temperature $T_{sub} \geq 600$ K, they are semi-metals (HA^{hot}).

In the present article, using HART as a weak ferromagnet in case of the F2-layer, and HA^{hot} as semi-metal in case of the F1-layer in structures F1/F2/S, we performed a detailed analysis of the SSV effect for both types of heterostructures. At the same time, we carried out a complete theoretical interpretation of the observed SSV effects. Preliminary results of the work were published in articles [31–34].

2. Samples

Previously, in our F1/F2/S structures (for example, see [6,8,9,26,32]), we used — CoO_x as an antiferromagnetic (AF) layer. We used the antiferromagnetic layer to fix the direction of the magnetization vector of the F1-layer. However, CoO_x loses its antiferromagnetic properties if HA^{hot} is used as the F1-layer. When the substrate is heated to high temperatures, the CoO_x layer is destroyed and becomes ordinary ferromagnetic cobalt, which is not able to fix magnetization. In this regard, we decided to abandon the AF-layer for structures that include the HA^{hot} layer. In these F1/F2/S structures, we use the natural difference between the coercive forces of the F1- and F2-layers. Now, for such structures, the magnetization direction of the F1-layer is free, while that for the F2-layer is fixed. This was achieved due to the fact that the magnetization of the Ni layer is more difficult to be affected by an external magnetic field than the magnetization of the HA^{hot}-layer.

The design of the two types of F1/F2/S heterostructures studied is shown in Fig. 2. In the structures of the first type, CoO_x is used as the AF-layer, which fixes the magnetization of the Py (here, F1-layer). This allows us to rotate the magnetization direction of the weak ferromagnetic layer

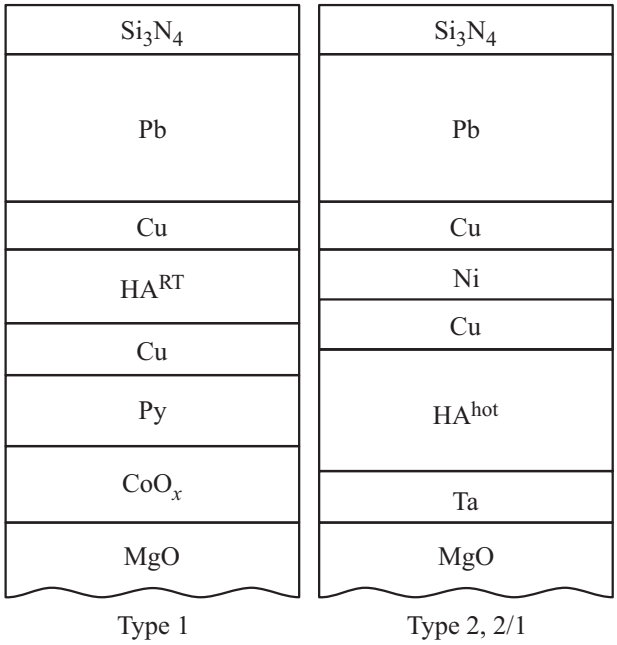

Figure 2. Three types of SSV structures studied in this article (see text for details).

HA^{RT} (here the F2-layer) by changing the direction of the applied external magnetic field. In turn, in the structures of the second type, the magnetization direction of HA^{hot} is free (here the F1-layer), and the magnetization direction of the Ni layer (here the F2-layer) is fixed due to the large coercive field. For the structures of the second type, the Ta layer is a buffer layer for the growth of HA^{hot}. The Cu layer between the F2-layer and the C-layer prevents mutual diffusion during the growth of SSV [35]. The Cu layer between two F-layers is necessary to separate the magnetizations of these layers.

It should be noted that these two types of sample structures were prepared at the sputtering plant of the Institute of Solid State (IFW Dresden) in Dresden, Germany. In 2021, we managed to transport this sputtering equipment from Germany to Russia. On this equipment, a series of samples of the 2/1 type was prepared at the Zavoisky Physical-Technical Institute (see the text below). The experimental results for this series are also presented in this article.

The samples were prepared on high-quality single-crystal MgO (001) substrates using the classical method of electron-beam evaporation in ultrahigh vacuum (of order of $1 \cdot 10^{-8}$ mbar (in Germany) and order of $1 \cdot 10^{-9}$ mbar (in Russia)) and magnetron sputtering in a closed vacuum cycle. The layers thickness during growth was controlled using a standard quartz thickness gage. All materials used for sample preparation were of purity above 4N, which corresponds to a contamination level of 0.01 at.%. The substrates were fixed on a special rotating sample holder, which enables to fabricate up to 8 samples in one vacuum cycle. Then, the sample holder was placed in the loading chamber. The Co, Ta, Py, Cu, Ni, and Pb layers were sputtered using the electron-beam evaporation method. The HA and Si_3N_4 layers were sputtered using the magnetron sputtering method.

The cobalt oxide was sputtered in two stages. First, Co was sputtered onto the substrate, then the substrate was moved to a loading lock and kept for 2 hours in an oxygen atmosphere at a pressure of 100 mbar. After the oxidation procedure, the sample holder was moved to the main chamber, where the sputtering process for the remaining layers continued. At the last stage, the sample holder was moved to the chamber for preparing layers using magnetron sputtering, where the samples were covered with a protective dielectric layer of silicon nitride Si_3N_4 85 nm thick to prevent oxidation of the Pb layer. To prepare high-quality Pb layers, high sputtering rates of the order of 1.0−1.2 nm/s were used. This was necessary to improve the transport properties of the lead layer. For other materials, we used the following sputtering rates: 0.037 nm/s for HA and 0.05 nm/s for Co, Cu, Ni, Ta, and Py layers. To optimize the growth of the upper SSV fragment containing the Pb layer after sputtering of the HA layer, we lowered the substrate temperature to 150 K, after which we continued the sample preparation process, as shown in our article [36]. Decreasing the substrate temperature reduces the roughness of the lead layer, thereby increasing the magnitude of the SSV effect. The parameters of the studied samples are given in the table.

It should be noted that the most important difference between structures of type 1 and 2 is the growth temperature of the $HA = Co_2Cr_{1-x}Fe_xAl_y$ layer, and between types 2 and 2/1 structures is the localization of the preparation place.

3. Experimental results

The magnetic properties of the spin valve structures were characterized using a Quantum Design 7T VSM SQUID magnetometer. First, samples of the 1 structure were cooled from room temperature to 10 K in the presence of a magnetic field +6 kOe applied in the plane of the sample. After such a cooling procedure, the magnetization of the Py layer turned out to be fixed due to the anisotropy field of the cobalt oxide layer AF, since the Neel temperature CoO_x is about 250−290 K. At a temperature of 10 K, the magnetic field changed from +4 kOe to −6 kOe and vice versa. The value of the magnetic moment lying in the plane of the sample was measured. For a sample of structures of type 1 PL34-81, the magnetization of the free layer HA^{RT} begins to decrease as the field decreases from +4 kOe to a field of the order of +0.1 kOe. At the same time, the magnetization of the Py layer remains fixed up to −2 kOe due to fixing by the CoO_x antiferromagnetic layer. Thus, in the field range from +0.1 to −2 kOe, the mutual orientation of two ferromagnetic layers is antiparallel. With a further change in the field from −2 to −2.5 kOe, the magnetization of the Py layer becomes free and begins to rotate in the direction of the applied external magnetic field. The small magnetic

Parameters of the studied samples presented in Fig. 2

Structure type	Sample name	d_{HA} (nm)	d_{Ni} (nm)
1	PL34-81	0.6	–
	PL34-18	1	–
	PL34-16	4	–
2	PLAK42-12	–	0.9
	PLAK42-14	–	1.6
	PLAK42-15	–	2.0
	PLAK42-16	–	2.5
2/1 — Kazan series	PLAK42-31	–	1.6
	PLAK42-32	–	2
	PLAK42-33	–	2.5
	PLAK42-34	–	3

Note.
Type 1: CoO_x(3.5 nm)/Py(5 nm)/Cu(4 nm)/HA^{RT}(dHA)/Cu(1.5 nm)/Pb(80 nm);
Type 2: Ta(5 nm)/HA^{hot}(20 nm)/Cu(4 nm)/Ni(dNi)/Cu(1.5 nm)/Pb(105 nm);
Type 2/1: Ta(5 nm)/HA^{hot}(20 nm)/Cu(4 nm)/Ni(dNi)/Cu(1.5 nm)/Pb(110 nm).

hysteresis loop for this sample showed that the external magnetic field ± 1 kOe is sufficient to change the mutual orientation of the magnetizations of F-layers from *P* to *AP*. Such a behavior of the magnetic properties is characteristic of the entire series of samples of type 1 structures.

Studies of the magnetic properties of type 2 structures have shown that saturation of the magnetization of the HA^{hot}layer occurs at 30 Oe. With a further increase in the magnetic field to 3 kOe, the magnetization slightly increases. The magnetic response from the Ni layer is not visible due to the relatively small value of the magnetic moment of this layer. Structures of the 2/1 type showed similar magnetic properties.

Measurements T_c were carried out by recording superconducting transitions by changing the resistance using the standard 4-x contact method at direct current on a setup that was created on the basis of the X-range EPR spectrometer by Bruker. It contains a vector electromagnet with a residual magnetic field of about 30 Oe, which enables to control the magnitude of the magnetic field with high accuracy during the experiment. The use of an electromagnet also greatly simplifies the procedure for rotating the sample in an external magnetic field applied in the plane of the sample. Before each measurement, a special procedure was carried out for adjusting the sample relative to the axis of rotation in order to minimize the magnetic field component perpendicular to the plane of the sample. The sample positioning error did not exceed several degrees relative to the direction of the external magnetic field. The magnetic field was measured using a Hall sensor with an accuracy of ± 0.3 Oe. The sample temperature was controlled using an Allen-Bradley carbon resistor with a nominal value of 230 Ω, which is the most sensitive in the temperature range of interest to us.

The quality of the Pb layer was controlled by the value of the electrical resistance ratio

$$RRR = R(300\,\mathrm{K})/R(10\,\mathrm{K}) = [\rho_{ph}(300\,\mathrm{K}) + \rho(10\,\mathrm{K})]/\rho(10\,\mathrm{K}),$$

where $R(T)$ is resistance measured at temperature T, $\rho_{ph}(300\,\mathrm{K})$ is phonon contribution to resistivity at a temperature of 300 K, and $\rho(10\,\mathrm{K})$ is residual resistance at a temperature of 10 K (above T_c). For all samples, *RRR* was between 10^{-12}, which is an indication of the high quality of the films. The magnitude T_c was determined as the middle of the superconducting transition. In zero magnetic fields, the widths of the superconducting transition curves varied from 20 to 50 mK from sample to sample and increased to 250 mK upon application of an external magnetic field.

The next necessary step was to determine the optimal thickness of the Pb-layer to observe the S/F proximity effect for structures of all types. The thickness of the Pb-layer should be small enough for the C-layer to be sensitive to the magnetic part of the system. Only in this case, the mutual orientation of the magnetizations of F1- and F2-layers will affect the magnitude T_c in the entire SSV structure. In order to determine the optimal thickness of the Pb-layer, we studied the dependences T_c on the thickness of the Pb-layer d_{Pb} in the structures HA^{RT}(12 nm)/Cu(1.5 nm)/Pb(d_{Pb}) for the samples of type 1 and Ni(5 nm)/Cu(1.5 nm)/Pb(d_{Pb}) for the samples of type 2. We used HA^{RT} layers with thickness $d_{HA} = 12$ nm and Ni with thickness $d_{Ni} = 5$ nm, which significantly exceed the depth of penetration of the Cooper pairs into these layers. At larger layer thicknesses, Pb T_c slowly decreases with decreasing d_{Pb} in both types of structures. The

value T_c starts to decrease sharply below $d_{Pb} \sim 60$ nm for HA^{RT}/Cu/Pb and $d_{Pb} \sim 130$ nm for Ni/Cu/Pb. Below $d_{Pb} \sim 30$ nm for HA^{RT}/Cu/Pb and below $d_{Pb} \sim 80$ nm for Ni/Cu/Pb T_c is less than 1.5 K. At small thicknesses d_{Pb}, the widths of superconducting transitions ∂T_c become extremely large (the order of 0.4 K). Taking into account that the influence of the magnetic part becomes stronger at small thicknesses of the Pb layer, we determined the optimal thicknesses of the lead layer $d_{Pb} = 80$ nm for the structures of type 1 and $d_{Pb} = 105-110$ nm for the structures of type 2 and 2/1.

3.1. Structures of type 1

To study the angular dependence T_c on the mutual orientation of the magnetizations of the F-layers, we used the same measurement protocol that had been used to study the magnetic properties of the samples on a 7T VSM SQUID magnetometer. According to the magnetic measurements P and AP, the mutual orientations of the magnetizations of the F-layers are achieved at fields $H_0 = +1$ and -1 kOe, respectively. For the samples of type 1 structures, the maximum magnitude ΔT_c^{full} is reached when the mutual orientation of the magnetizations changes from collinear to orthogonal and amounts to ~ 0.05 K (see Fig. 3).

For a series of samples of type 1 structures with different thicknesses d_{HA}, we studied the dependence T_c on the angle α between the direction of the frozen field and the external magnetic field applied along the plane of the sample. As can be seen in Fig. 4, when the mutual orientation of the magnetizations changes by smoothly rotating the magnetic field from the P ($\alpha = 0°$) state to the AP ($\alpha = 180°$) state, T_c changed non-monotonically and passed through a minimum near the orthogonal orientation of the magnetizations. According to theory [7], the characteristic minimum in the dependence $T_c(\alpha)$, which is most pronounced near $\alpha = 90°$, unambiguously indicates the generation of LRTC in the superconducting condensate in structures F1/F2/S. If we assume that there is no triplet component (although, according to the theory, their occurrence is inevitable), we can expect that the dependence $T_c(\alpha)$ will be monotonic. Based on general considerations, T_c should be a function α^2 and $(\pi - \alpha)^2$ as the angle changes from 0 to π. Thus, the dependence $T_c(\alpha)$ can be expressed in terms of T_c^P and T_c^{AP} as follows: $T_c^{ref}(\alpha) = T_c^P \cos^2(\alpha/2) + T_c^{AP} \sin^2(\alpha/2)$.

This curve is represented by a dashed line in Figs. 4, 7 and 10. Let's call these curves reference curves. The deviation of the actual value T_c from this reference curve demonstrates the contribution of LRTC to the magnitude of the spin valve effect.

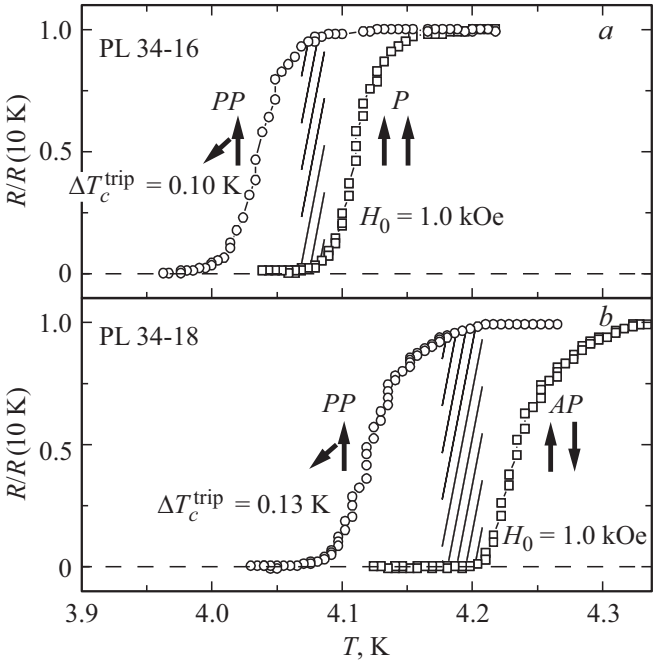

Figure 3. Superconducting transition curves for different mutual orientations of the magnetizations of F-layers in an external magnetic field $H_0 = +1$ kOe for two samples: (a) sample PL34-16 (for P and PP) and (b) sample PL34-18 (for AP and PP). The dashed rectangle $\Delta T_c^{full} \sim 0.05$ K shows the working area of SSV.

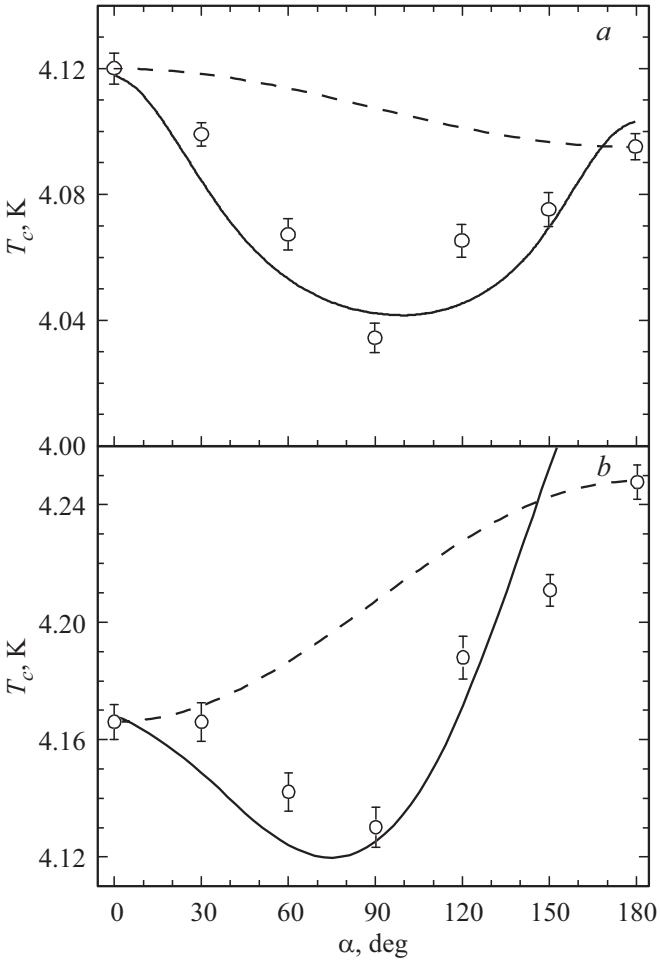

Figure 4. Angular dependences $T_c(\alpha)$ measured in an external magnetic field $H_0 = +1$ kOe: (a) PL34-16 and (b) PL34-18. Reference curves are shown by a dashed line. Theoretical curves constructed according to the theory of Fominov et al. in article [34] are shown with a solid line.

From Fig. 4, *a*, which shows the angular dependence T_c for the sample PL34-16, we obtain the value of the SSV singlet effect $\Delta T_c = -25$ mK. The negative sign of the effect magnitude means that we observe the reverse SSV effect, due to the destructive quantum interference of the pair wave function of the Cooper pair. From Fig. 4, *b*, which shows the angular dependence T_c for the sample PL34-18, we obtain the value of the SSV singlet effect $\Delta T_c = +85$ mK. A positive effect size corresponds to a direct SSV effect. As can be seen in Fig. 4, *b*, $\Delta T_c^{\text{trip}} = T_c^P(\alpha = 0°) - T_c^{PP}(\alpha = 90°)$ is about 100 mK. In this case, the magnitude of the SSV effect when the mutual orientation of the magnetizations changes from *AP* to *PP* exceeds the width of the superconducting transition ∂T_c=70 mK. Therefore, for the sample PL34-18 there is a possibility of complete switching between the normal and superconducting states by changing the mutual orientation of magnetizations of F-layers from *AP* to *PP*. Indeed, we managed to carry out a complete switching from the working area of the SSV $\Delta T_c^{\text{full}} \sim 0.05$ K (see Fig. 3). This magnitude is still not very large, but still exceeds five times the magnitude obtained in our first article [6].

3.2. Structures of type 2

According to our magnetic measurements for samples of type 2 structures, initially, we believed that to control the magnetization direction of the HA^{hot}-layer a magnetic field of 30 Oe would be sufficient, since the magnetization of the HA^{hot}-layer is already saturated in this field. We carried out such experiments and found the value of the SSV effect, which is standard for us, $\Delta T_c = 0.1$ K in a field of 0.5 kOe. Then, just out of curiosity, we conducted studies of the SSV magnitude in higher magnetic fields. We discovered an effect that was surprising for us — with the increasing magnetic field, the triplet contribution to the magnitude of the SSV effect increased linearly. For example, for the sample PLAK42-16 ΔT_c^{trip} increases linearly to 0.4 K in a field of 2 kOe (see Fig. 5).

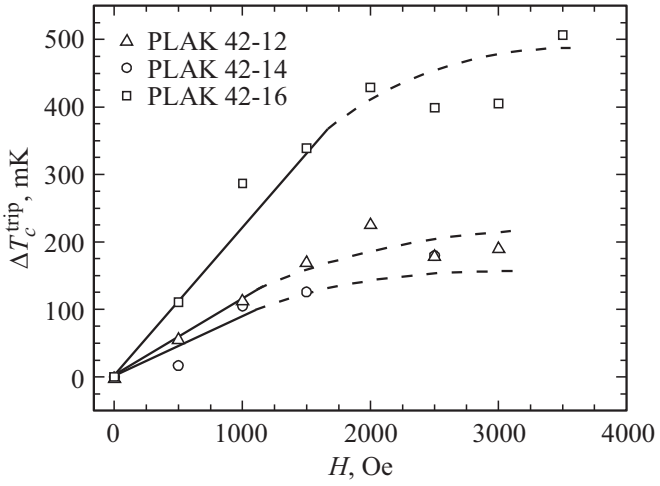

Figure 5. Dependence of the magnitude of the SSV ΔT_c^{trip} triplet effect on the external magnetic field H for three different samples of type 2 structures. Solid line is an eye guide.

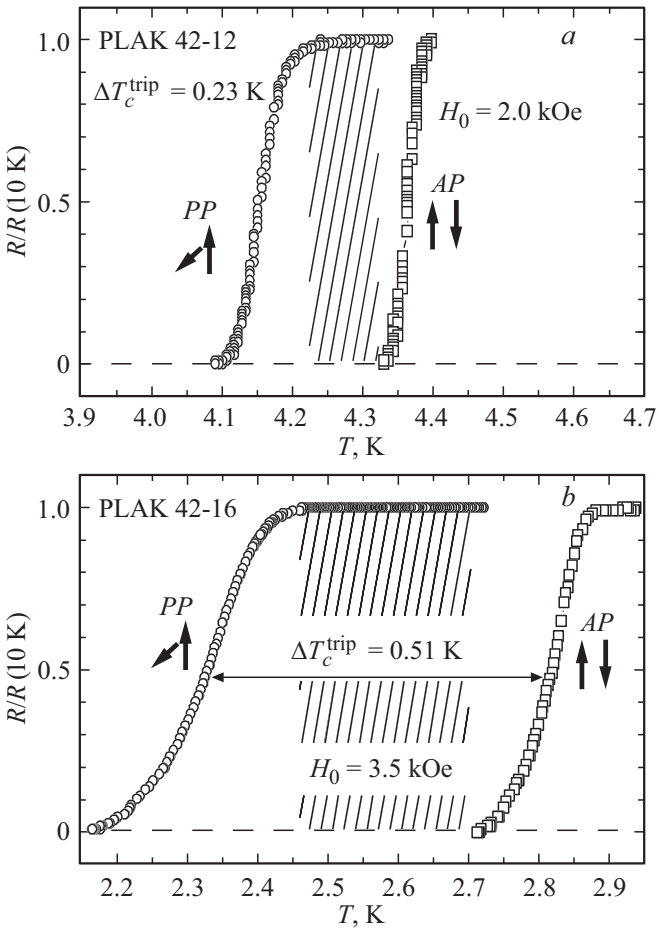

Figure 6. Curves of superconducting transitions for different mutual orientations of the magnetizations of F-layers: (*a*) PLAK 42-12 sample (for *AP* and *PP*) in an external magnetic field $H_0 = +2$ kOe; (*b*) is a record difference in the curves of superconducting transitions measured with parallel and perpendicular orientations of the magnetizations of ferromagnetic layers in an external magnetic field $H_0 = +3.5$ kOe for the PLAK42-16 sample. The dashed rectangle $\Delta T_c^{\text{full}} \sim 0.3$ K shows the working area of SSV.

It should be noted that a similar increase ΔT_c^{trip} was observed by Singh et al. in [29]. Obviously, this field-dependent effect, observed by the two groups on different samples, is a very important discovery, since it seems to be a characteristic feature of new types of SSV with semi-metallic layers and requires a theoretical explanation. The maximum difference in T_c between the *P* and *PP* orientations of the F1- and F2-layers magnetizations is $\Delta T_c^{\text{trip}} \sim 0.51$ K for the sample PLAK42-16 (see Fig. 6, *b*). The magnitude ΔT_c^{trip} for the entire series of samples is in the range from 0.18 to 0.51 K (see Fig. 5).

Fig. 7 shows the dependences T_c on α for two samples. The behavior of the dependence $T_c(\alpha)$ qualitatively coincides with the angular dependences that were observed earlier in our articles [9,26,32]. However, here we observe a huge dip in the values of T_c for the orthogonal orientation of the magnetizations of F1- and F2-layers, which was not

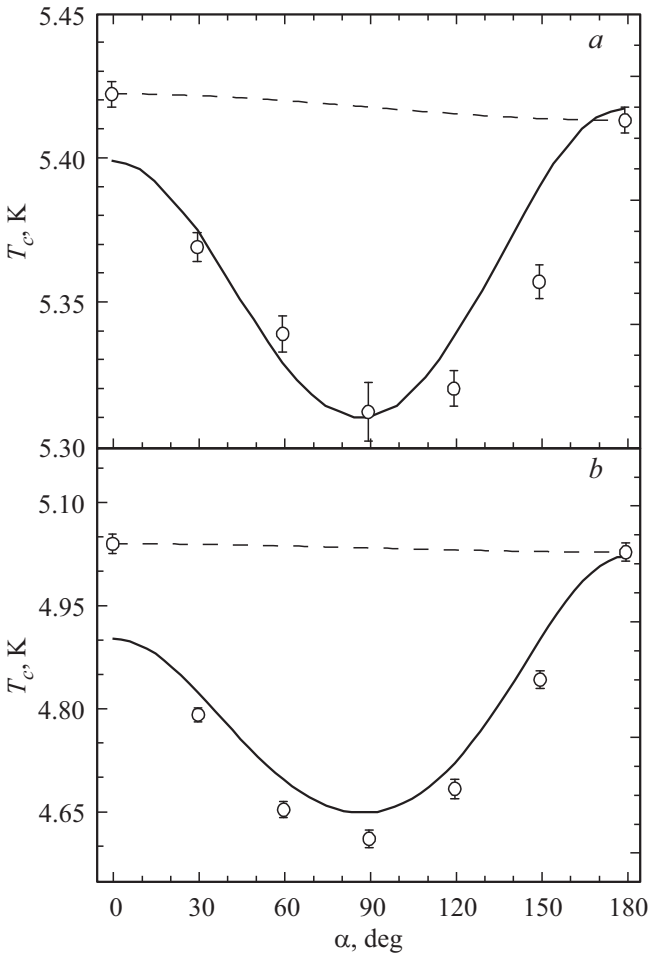

Figure 7. Angular dependences $T_c(\alpha)$ measured in an external magnetic field $H_0 = +1$ kOe: (*a*) PLAK42-12 and (*b*) PLAK42-16. Reference curves are shown by a dashed line. Theoretical curves constructed according to the theory of Fominov et al. in article [34] are shown with a solid line.

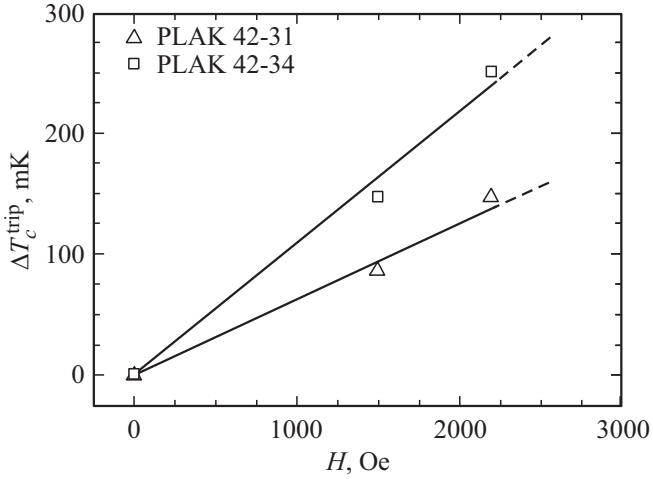

Figure 8. Dependence of the magnitude of the SSV ΔT_c^{trip} triplet effect on the external magnetic field H for two different samples of type 2/1 structures. Solid line is an eye guide.

observed before. This suggests that Cooper pairs with triplet spin polarization dominate in the SSV effect. Indeed, according to Fig. 7, the singlet contribution to the SSV effect is practically negligible. For the samples of type 2 structures, which exhibit a huge magnitude of the SSV effect, we observe an increase in ∂T_c for the PP orientation of the magnetizations (see Fig. 6). In addition, the magnitude of the triplet SSV effect ΔT_c^{trip} depends on the applied magnetic field up to a certain value, which is different for different samples (see Fig. 5).

3.3. Structures of type 2/1

This series of samples was prepared for adjusting the operation of sputtering equipment in Kazan. For this series of samples, the effect of an increase in the triplet contribution to the SSV effect magnitude with increasing the magnetic field was also found (see Fig. 8). For example, for the sample PLAK42-4 ΔT_c^{trip} increases linearly to 0.25 K in a field of 2.2 kOe (see Fig. 8).

It should be noted that a similar increase ΔT_c^{trip} was also observed for the samples of type 2 structures (see Fig. 5). This fact, firstly, allows us to state that the sputtering plant reached its operating parameters after moving from Germany, and secondly, it shows that the linear increase ΔT_c^{trip} on the magnitude of the magnetic field is a characteristic feature of new types of SSVs with semi-metallic layers and requires a theoretical explanation. The maximum difference in T_c between the P and PP orientations of the F1- and F2-layers magnetizations is $\Delta T_c^{trip} \sim 0.25$ K for the sample PLAK42-34 (see Fig. 9).

Fig. 10 shows the dependences T_c on α for two samples of 2/1 type structures. The behavior of the dependence $T_c(\alpha)$ qualitatively coincides with the angular dependences obtained for the samples of type 2 structures.

4. Discussion of results

The theoretical curves shown in Figs. 4 and 7 were constructed according to the theory of Fominov et al. [7]. The extended theory in the appendix to our article [34] allows us to consider our heterostructures with different layer material parameters and arbitrary Kupriyanov–Lukichev boundary parameters [37] of all F1/F2/S interfaces. Each of the two interfaces (F2/S and F1/F2) is described by the boundary materials parameter γ and the boundary transparency parameter γ_b [34]. It can be seen in Figs. 4 and 7 that the theory reproduces well the characteristic features of the dependence $T_c(\alpha)$. The parameters of the studied F1/F2/S heterostructures, which we used for theoretical calculations for the structures of types 1 and 2, are presented in section 6 of our article [34].

4.1. Structures of type 1

As a rule, switching of the superconducting current in SSV structures was carried out by changing the mutual

orientation of the magnetizations of the F-layers from AP to P, or by combining the singlet and triplet SSV effects. In our type 1 structures for two different samples, complete switching was achieved by changing the mutual orientations of the magnetization between AP and PP. It should be noted that for the sample PL34-16 the difference $T_c^{AP} - T_c^{P}$ was 60 mk, which is almost 2 times less than the difference $T_c^{P} - T_c^{PP}$ equal to 100 mK. Thus, the main role in switching the superconducting current was played by the triplet contribution to the SSV effect.

4.2. Structures of type 2

The huge difference in the curves of superconducting transitions measured for the parallel and perpendicular magnetization orientations of the ferromagnetic layers for the sample PLAK42-16 in Fig. 6 indicates the dominant spin-triplet correlations of the superconducting condensate in our samples of type 2 structures. Fig. 7 demonstrates that the theory qualitatively and quantitatively reproduces the

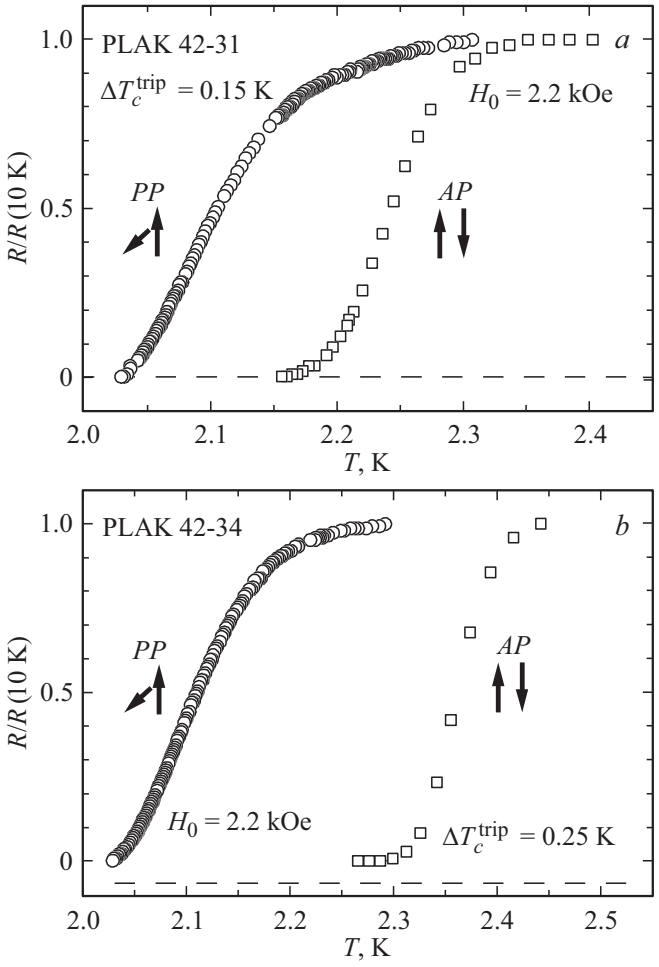

Figure 9. Curves of superconducting transitions measured at antiparallel and perpendicular orientations of the magnetizations of ferromagnetic layers in an external magnetic field $H_0 = +2.2$ kOe for two samples: (a) sample PLAK42-31 and (b) sample PLAK42-34.

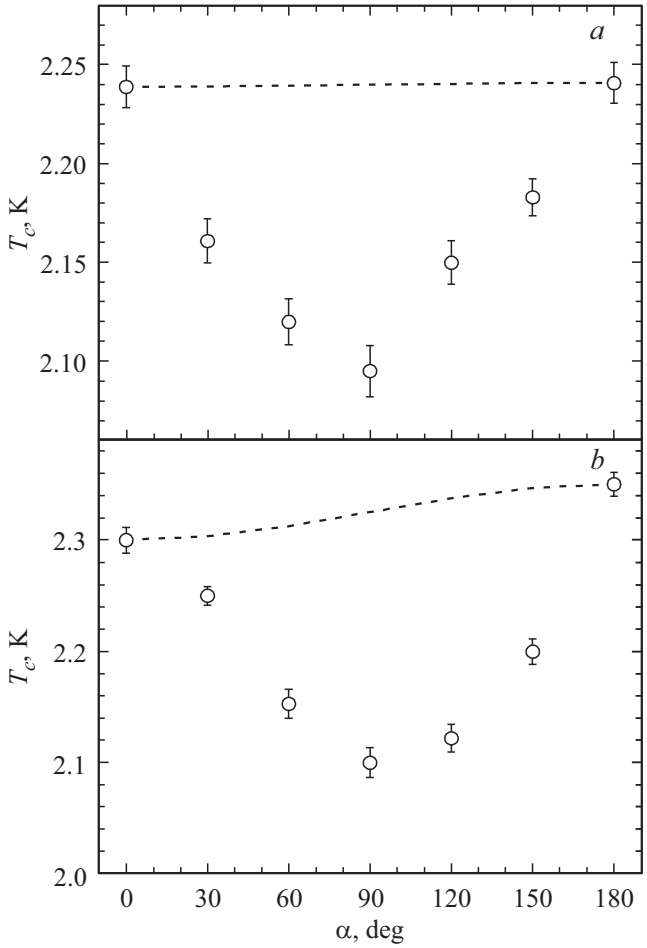

Figure 10. Angular dependences $T_c(\alpha)$ measured in an external magnetic field $H_0 = +2.2$ kOe: (a) sample PLAK42-31 and (b) sample PLAK42-34. Reference curves are shown by a dashed line.

characteristic features of the dependence $T_c(\alpha)$. In Fig. 6, it can be seen that the working area of the sample PLAK42-16 is $\Delta T_c^{full} \sim 0.3$ K. This value is 30 times greater than what was obtained in our first samples [6] and 1.5 times greater than in Singh et al. [29]. As can be seen in Figs. 5 and 8, the value ΔT_c^{trip} increases linearly with an increase in the applied external magnetic field. At first glance, it seems surprising that the magnitude of the triplet contribution to the magnitude of the SSV ΔT_c^{trip} effect increases at fields significantly higher than the magnetization saturation field of the HA^{hot} layer. As one, but not the only, possible cause, Singh et al. in article [29] suggested that this is due to the magnetic heterogeneity of the semi-metallic ferromagnetic layer. In our case, this is the HA^{hot} layer, which also apparently has a magnetic heterogeneity, as evidenced by a slight increase in its magnetization up to a field of 3 kOe, when more and more „microdomains“ are involved in the total magnetic moment of the layer. The experimental results obtained show that, as a result of the optimal selection of materials for the F-layers, the triplet contribution probably always dominates in the SSV

effect. According to the results of this article and the data of article [29], it follows that semi-metallic compounds are most likely the best materials known at the moment for the F1-layer in the SSV F1/F2/C structures. Such a high efficiency of a semi-metal is due to the fact that electrons incident on its surface can penetrate it only when they have a certain direction of the spin. This primarily applies to the spin-polarized Cooper pairs, which, depending on the direction of electron spins, will either be reflected from the S/F interface or penetrate deeply into it.

4.3. Structures of type 2/1

All the results obtained for the structures of type 2/1 agree qualitatively with the results obtained for the structures of type 2. For this type of structures, we observe a huge dip in the values of T_c for the orthogonal orientation of the magnetizations of the F1- and F2-layers (see Fig. 10). Here we succeeded in complete switching of the superconducting current by changing the mutual orientation of the magnetizations of the F-layers from *AP* to *PP* (see Fig. 9, *b*), where the key role was played by the Cooper pairs with triplet spin polarization, since the singlet contribution to the SSV effect is practically negligible (see Fig. 10, *b*). The results obtained for this type of samples, firstly, allow us to state that all the results for the structures of type 2 are qualitatively reproduced. Secondly, the sputtering plant has successfully moved from Germany to Russia, commissioning has been successfully carried out, the plant has reached its operating parameters.

5. Conclusion

We studied the structures of a superconducting spin valve, the magnetic part of which contains the Heusler alloy $Co_2Cr_{1-x}Fe_xAl_y$ with different degrees of spin polarization conduction zones. We have discovered a huge SSV effect $\Delta T_c^{\text{trip}} \sim 0.5\,\text{K}$, associated primarily with LRTC of the superconducting condensate, in an applied external magnetic field of the order of 3.5 kOe, which is significantly less than in the earlier articles [29]. Our observations indicate that the concept of SSV with a semi-metallic ferromagnetic material, proposed in article [29], is of a general nature. In particular, the search for the most suitable ferromagnetic material with a high degree of spin polarization of the conduction zone seems to be an extremely important task in order to achieve maximum values ΔT_c^{trip}. To date, we have already increased the working area of the SSV ΔT_c^{full} to 0.3 K, which is 30 times larger compared to the results observed in our first article [6] and 1.5 times larger than in Singh et al. [29]. In addition, it should be noted that the experimental results obtained by us in this article and in article [29] require a more detailed theoretical analysis. To date, the question remains why the triplet contribution to the magnitude of the SSV effect increases above the value of the magnetic saturation field of the semi-metallic layer.

Acknowledgments

The authors would like to thank I. Schumann, V. Kataev, and B. Buchner from the Solid State Institute (IFW), Dresden, for a constructive discussion.

Funding

The work of Ya.V. Fominov was carried out within the scope of the state assignment of the Landau Institute for Theoretical Physics of the Russian Academy of Sciences, and was also supported by a grant from the Foundation for the Development of Theoretical Physics and Mathematics BAZIS.

The work of A.A. Kamashev, I.A. Garifullin, N.N. Garifyanov, A.A. Validov was carried out within the scope of the state assignment of FRC KazSC of RAS.

Conflict of interest

The authors declare that they have no conflict of interest.

References

[1] L.B. Ioffe, V.B. Geshkenbein, M.V. Feigel'man, A.L. Fauchere, G. Blatter. Nature **398**, 679 (1999).
[2] M.V. Feigelman. UFN, **169**, 917 (1999) (in Russian).
[3] D.V. Ryazanov. UFN, **169**, 920 (1999) (in Russian).
[4] S. Oh, D. Youm, M.R. Beasley. Appl. Phys. Lett. **71**, 2376 (1997).
[5] L.R. Tagirov. Phys. Rev. Lett. **83**, 2058 (1999).
[6] P.V. Leksin, N.N. Garif'yanov, I.A. Garifullin, J. Schumann, H. Vinzelberg, V. Kataev, R. Klingeler, O.G. Schmidt, B. Büchner. Appl. Phys. Lett. **97**, 102505 (2010).
[7] Ya.V. Fominov, A.A. Golubov, T.Yu. Karminskaya, M.Yu. Kupriyanov, R.G. Deminov, L.R. Tagirov. JETP Lett. **91**, 329 (2010).
[8] P.V. Leksin, N.N. Garif'yanov, I.A. Garifullin, J. Schumann, V. Kataev, O.G. Schmidt, B. Büchner. Phys. Rev. Lett. **106**, 067005 (2011).
[9] I.A. Garifullin, P.V. Leksin, N.N. Garif'yanov, A.A. Kamashev, Ya.V. Fominov, J. Schumann, Y. Krupskaya, V. Kataev, O.G. Schmidt, B. Büchner. J. Magn. Magn. Mater. **373**, 18 (2015).
[10] M.G. Blamire, J.W.A. Robinson. J. Phys.: Condens. Matter **26**, 453201 (2014).
[11] J. Linder, J.W.A. Robinson. Nature Phys. **11**, 307 (2015).
[12] N.G. Pugach, M. Safonchik, T. Champel, M.E. Zhitomirsky, E. Lähderanta, M. Eschrig, C. Lacroix. Appl. Phys. Lett. **111**, 162601 (2017).
[13] Q. Cheng, B. Jin. Physica C **473**, 29 (2012).
[14] J. Zhu, I.N. Krivorotov, K. Halterman, O.T. Valls. Phys. Rev. Lett. **105**, 207002 (2010).
[15] X.L. Wang, A. Di Bernardo, N. Banerjee, A. Wells, F.S. Bergeret, M.G. Blamire, J.W.A. Robinson. Phys. Rev. B **89**, 140508(R) (2014).
[16] M.G. Flokstra, T.C. Cunningham, J. Kim, N. Satchell, G. Burnell, P.J. Curran, S.J. Bending, C.J. Kinane, J.F.K. Cooper, S. Langridge, A. Isidori, N. Pugach, M. Eschrig, S.L. Lee. Phys. Rev. B **91**, 060501(R) (2015).

[17] K. Dybko, P. Aleshkevych, M. Sawicki, P. Przyslupski. J. Magn. Magn. Mater. **373**, 48 (2015).
[18] D. Lenk, V.I. Zdravkov, J.-M. Kehrle, G. Obermeier, A. Ullrich, R. Morari, H.-A. Krug von Nidda, C. Müller, M.Yu. Kupriyanov, A.S. Sidorenko, S. Horn, R.G. Deminov, L.R. Tagirov, R. Tidecks. Beilstein J. Nanotechnol. **7**, 957 (2016).
[19] S. Voltan, A. Singh, J. Aarts. Phys. Rev. B **94**, 054503 (2016).
[20] Z. Feng, J.W.A. Robinson, M.G. Blamire. Appl. Phys. Lett. **111**, 042602 (2017).
[21] A. Srivastava, L.A.B. Olde Olthof, A. Di Bernardo, S. Komori, M. Amado, C. Palomares-Garcia, M. Alidoust, K. Halterman, M.G. Blamire, J.W.A. Robinson. Phys. Rev. Appl. **8**, 044008 (2017).
[22] E. Moen, O.T. Valls. Phys. Rev. B **95**, 054503 (2017).
[23] Zh. Devizorova, S. Mironov. Phys. Rev. B **95**, 144514 (2017).
[24] M. Alidoust, K. Halterman. Phys. Rev. B **97**, 064517 (2018).
[25] A.A. Jara, C. Safranski, I.N. Krivorotov, C.-T. Wu, A.N. Malmi-Kakkada, O.T. Valls, K. Halterman. Phys. Rev. B **89**, 184502 (2014).
[26] P.V. Leksin, N.N. Garif'yanov, A.A. Kamashev, A.A. Validov, Ya.V. Fominov, J. Schumann, V. Kataev, J. Thomas, B. Büchner, I.A. Garifullin. Phys. Rev. B **93**, 100502(R) (2016).
[27] J.Y. Gu, C.-Y. You, J.S. Jiang, J. Pearson, Y.B. Bazaliy, S.D. Bader. Phys. Rev. Lett. **89**, 267001 (2002).
[28] Y. Gu, G.B. Halász, J.W.A. Robinson, M.G. Blamire. Phys. Rev. Lett. **115**, 067201 (2015).
[29] A. Singh, S. Voltan, K. Lahabi, J. Aarts. Phys. Rev. X **5**, 021019 (2015).
[30] A.A. Kamashev, P.V. Leksin, J. Schumann, V. Kataev, J. Thomas, T. Gemming, B. Büchner, I.A. Garifullin. Phys. Rev. B **96**, 024512 (2017).
[31] A.A. Kamashev, N.N. Garifyanov, A.A. Validov, I. Schumann, V. Kataev, B. Byukhner, Ya.V. Fominov, I.A. Garifullin. Pisma v ZhETF **110**, 325 (2019) (in Russian).
[32] A.A. Kamashev, P.V. Leksin, N.N. Garif'yanov, A.A. Validov, J. Schumann, V. Kataev, B. Büchner, I.A. Garifullin. J. Magn. Magn. Mater. **459**, 7 (2018).
[33] A.A. Kamashev, N.N. Garif'yanov, A.A. Validov, J. Schumann, V. Kataev, B. Büchner, Ya.V. Fominov, I.A. Garifullin. Beilstein J. Nanotechnol. **10**, 1458 (2019).
[34] A.A. Kamashev, N.N. Garif'yanov, A.A. Validov, J. Schumann, V. Kataev, B. Büchner, Ya.V. Fominov, I.A. Garifullin. Phys. Rev. B **100**, 134511 (2019).
[35] P.V. Leksin, N.N. Garif'yanov, A.A. Kamashev, Ya.V. Fominov, J. Schumann, C. Hess, V. Kataev, B. Büchner, I.A. Garifullin. Phys. Rev. B **91**, 214508 (2015).
[36] P.V. Leksin, A.A. Kamashev, J. Schumann, V.E. Kataev, J. Thomas, B. Büchner, I.A. Garifullin. Nano Res. **9**, 1005 (2016).
[37] M.Yu. Kupriyanov, V.F. Lukichev. ZhETF **94**, 139 (1988) (in Russian).